Desalination and Water Treatment
www.deswater.com

doi: 10.1080/19443994.2014.937761

56 (2015) 388–398
October

Development of a four-layered ANN for simulation of an electrochemical water treatment process

Hadi Rezaei Vahidian[a,*], Ali Reza Soleymani[b,*], Jalal Basiri Parsa[c]

[a]*Department of Chemistry and Chemical Engineering, Malek Ashtar University of Technology, Tehran, Iran, Tel. +98 851 3339843; email: hrvahidian_1984@yahoo.com*
[b]*Faculty of Science, Department of Applied Chemistry, Malayer University, Malayer 65719, Iran, Tel. +98 851 3339843; email: a.r.soleymani@malayeru.ac.ir*
[c]*Department of Applied Chemistry, Bu-Ali Sina University, Hamadan, Iran, Tel. +98 811 8282807; email: parssa@basu.ac.ir*

Received 28 January 2014; Accepted 16 June 2014

ABSTRACT

This work is dealing with the performance and modeling of an electrochemical water treatment process. A bench-scale electrochemical reactor with working volume of 0.5 L was applied to treat an azo dye, acid brown 14, as a typical pollutant in aqueous media. For the dye initial concentration of 50 mg/L, the experimental data showed the optimum conditions of the process as: [NaCl] = 5 g/L, pH 6.4, and $V = 4$ V. Under the conditions, after 18 min and consuming of low energy amount of 0.24 Wh/L, 92% of decolorization efficiency (DE) was obtained. To model the process and simulate the obtained results, artificial neural network (ANN) method was used. Five effective operational parameters, i.e. reaction time, initial pH, applied voltage, supporting electrolyte, and the dye initial concentrations were considered as the network inputs; meanwhile, both of the DE and energy consumption (EC) criteria, were considered as the relevant network outputs. A four-layered feed-forward ANN, consisting of "trainbfg" learning algorithm and "tansig" as the transfer function in both hidden and output layers, was constructed. The neuron number structure of 5:4:6:2 and the iteration number of 600, showed best model-calibration ability. The K-fold cross-validation method showed high correlation coefficients (R^2) of 0.988 and 0.983 for the simulation of the DE and EC criteria, respectively.

Keywords: Modeling; Four-layered ANN; Electrochemical oxidation; K-fold cross validation

1. Introduction

Dyestuff effluent is one of the industrial wastewaters that are difficult to be treated because of the intensive color, high organics content, variable pH, and temperature as well as low biodegradability [1–5]. There are many processes to remove the dyes from effluents, such as: adsorption by activated carbon [6], coagulation and electrocoagulation [7,8], photo catalytic degradation [9], fenton, electro fenton, photo fenton, and ozonation [10–13]. In recent years, there has been increasing interest on the use of electrochemical methods for the wastewater treatment, since the main consumed reagent is the electron and also there is no need to add any chemicals into the media [3,14–18]. In the electro-oxidation (EO) process, organic pollutants are destroyed by either direct or indirect anodic

---

*Corresponding authors.

oxidation. In the direct oxidation, pollutants are first adsorbed on the anode surface and then destroyed by anodic electron transfer reactions [19]. For the indirect oxidation, strong oxidants such as hypochlorite and chlorine are generated electrochemically and then attack the pollutants in the media (Eqs. (1–5)) [12]. The other advantages of the EO process are the *in situ* generation of the all active oxidants and their immediate consumption. In addition, the practical optimization of the EO process is precisely performable, and the process is conducted easily at its optimum conditions via a controlling system.

$$Cl^- \rightleftharpoons Cl^{\cdot}_{ads} + e^- \quad (1)$$

$$Cl^- + Cl^{\cdot}_{ads} \rightleftharpoons Cl_2 + e^- \quad (2)$$

$$Cl_2 + H_2O \rightarrow HOCl + H^+ + Cl^- \quad (3)$$

$$HOCl \rightarrow H^+ + OCl^- \quad (4)$$

$$Dye + OCl^- \rightarrow intermediate \rightarrow CO_2 + Cl^- + H_2O \quad (5)$$

In so many cases, application of a control system to assess the process performance automatically would lead to quick identification and correction of the source of any controlling problems. This proceeding is possible if an appropriate model be existed to simulate the process adequately well. In fact, a model can give some information about the possibility of the process outcomes based on the observed incomes. Also, modeling of a process enables us to avoid repetitive experimentation and time waste [20]. Some techniques, such as statistical methods and artificial neural networks (ANNs) can be applied to make convenient models for different processes [21]. Generally, since the EO process depends on several factors, modeling of it is somewhat complicated. Therefore, simple linear multivariate correlation cannot model the process satisfactorily. During the last decade, ANNs have been attracting great interest as predictive models in water and wastewater treatment [22–24]. They are computer-based systems, which have been designed to simulate the learning process of the human brain neurons. They have an ability to "learn" based on a set of experimental data (e.g. processing conditions and corresponding responses) without any knowledge about the physical and chemical laws that govern the process. This is one of the main benefits of ANNs, compared with empirical and statistical methods. In this regard, feed-forward back propagation ANNs are the most often used to map input–output relationships in different cases [25].

The present research studies the practical performance as well as modeling of an EO process, dealing with decolorization of an azo dye, Acid Brown 14 (AB14), in aqueous media. The process operation was optimized considering to the several important independent factors, such as reaction time, initial pH, applied voltage, supporting electrolyte amount, and initial concentration of the pollutant. Also, decolorization efficiency (DE) and energy consumption (EC) of the process were selected as dependent factors. In order to find the best model, several different three- and four-layered feed-forward back-propagation networks were designed and optimized. Moreover, to examine the reliability of the best model, K-fold cross validation method was applied.

2. Experimental

2.1. Reagents

The azo dye, AB14, was supplied from Alvan Sabet Company, with purity of 99% that its characteristics have been presented in Table 1. Sodium hydroxide and sulfuric acid, sodium chloride (supporting electrolyte), potassium dichromate and ferrous ammonium sulfate (applied to assess chemical oxygen demand [COD]), and 1,10-phenanthroline and ferrous sulfate (used to prepare ferroin indicator solution) were all Merck products.

2.2. Electrochemical cell

The experiments were performed in a bench-scale electrochemical cell with a working volume of 0.5 L. The cell was equipped with one platinum plate (2 cm × 2 cm) as the anode, placed in the middle of the cell, and two stainless steel plates (SS-304) as the cathodes (2 cm × 8 cm), placed at the both sides of the central anode. Here, the cathodes act as the auxiliary and the anode acts as the working electrode. For the auxiliary electrode, it is often preferred to possess a surface area much larger than that of the working electrode to ensure that the half reaction occurring at the auxiliary electrode is occurred fast enough so that it do not limit the process at the working electrode.

DC power supply (ADAK, PS-405) was used to apply voltage to the electrochemical cell. A schematic view of the experimental setup has been shown in Fig. 1.

2.3. Procedure and analysis

All experiments were performed at ambient temperature and mixing of the cell was provided using a

Table 1
The characteristics of AB 14

Molecular structure	Molecular formula	M_w (g mol^{-1})
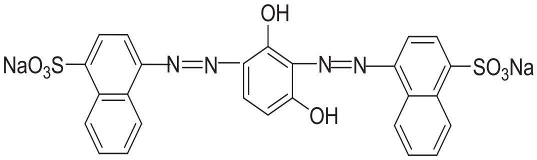	$C_{26}H_{16}N_4Na_2O_8S_2$ C.I. no.: 20195	622.54

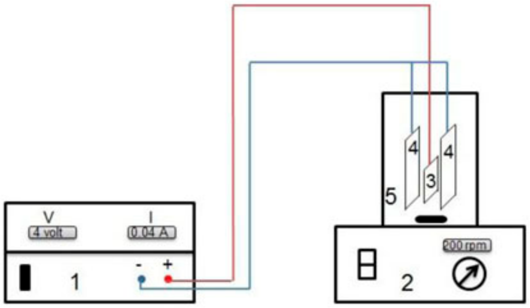

Fig. 1. Schematic diagram of the electrochemical cell; (1) DC power supply, (2) magnetic stirrer, (3) anode, (4) cathode, and (5) electrochemical cell.

magnetic stirrer. Solutions with the certain amounts of the dye and supporting electrolyte, after adjustment of pH using concentrated solutions of H_2SO_4 or NaOH, were transferred into the cell. After starting the electrolysis process, samples (4 mL) were taken at regular time intervals. The residual dye concentration was analyzed by a spectrophotometer (Perkin–Elmer, 55 OSE) via measurement of the solution absorbance at maximum wavelength of 461 nm, based upon appropriate calibration curves. The DE was calculated as follow:

$$\mathrm{DE} = \frac{[\mathrm{AB14}]_0 - [\mathrm{AB14}]_t}{[\mathrm{AB14}]_0} \tag{6}$$

where $[\mathrm{AB14}]_0$ and $[\mathrm{AB14}]_t$ are the initial and residual concentrations of the substrate, respectively.

COD was determined by the open reflux method according to the standard method procedure. In this method, the sample is refluxed in strongly acid solution with a known excess amount of potassium dichromate ($K_2Cr_2O_7$). In this condition, all organic substances are oxidized to CO_2; meantime, the Cr^{6+} is reduced to Cr^{3+}. After 2-h reflux at 150˚C, the remaining of $K_2Cr_2O_7$ is titrated with ferrous ammonium sulfate, in the presence of ferroin as an indicator. Hence, the amount of consumed $K_2Cr_2O_7$ is determined and the oxidizable organics are calculated in terms of oxygen equivalent [26].

EC criterion, (in Wh) was calculated during the process according to Eq. (7):

$$\mathrm{EC} = VIt \tag{7}$$

where V is the cell potential (in volt), I is the induced current (in A), and t is the process time (in h).

2.4. ANN strategy

An ANN can be composed of several layers; the first layer is named as the input layer and the last layer is named as the output layer. Also, other layers that are located between these two layers are called hidden layers. In the present work, the process time, initial pH, applied voltage, NaCl concentration, and initial concentration of the dye were chosen as the input variables of the network. Meanwhile, the DE and EC were considered as the outputs of the network. The applied ranges of the inputs and outputs have been reported in Table 2. The structure of an ANN is determined by the number of its layers, number of neurons in each layer, and the nature of learning algorithm and transfer functions. The most important step in the development of an ANN model is the determination and optimization of its structure. In the work, the hidden neurons number and the

Table 2
The ranges of input and output parameters

Input layer parameter	Value	Output parameter	Value
Time (min)	0–30	DE	0–1
pH	2–10	EC	0–0.87
Voltage (volt)	2–6		
[NaCl] (mg/L)	2–7		
[AB14] (mg/L)	30–100		

Table 3
The components of the used ANN models

Model no.	Training algorithm	Transfer function	
		Hidden layer	Output layer
1	Trainscg	Tansig	Purelin
2	Trainscg	Tansig	Tansig
3	Trainbfg	Tansig	Purelin
4	Trainbfg	Tansig	Tansig
5	Trainlm	Tansig	Purelin
6	Trainlm	Tansig	Tansig

number of network calibration iterations were selected as the design parameters. Furthermore, application of an appropriate algorithm and a transfer function is necessary; otherwise, the model will not be reliable. Here, the performance of "tansig" and "purelin" transfer functions in the hidden and output layers were examined. Also, three different back propagation learning algorithms were used to train the networks. Hence, six different networks were structured and optimized, and their characteristics have been presented in Table 3. The MATLAB software (version 2009a) was utilized and all m-files were run by a personal computer.

2.5. Data pretreatment

Training or learning is the process of determining the weights of an ANN. The process minimizes the error function by setting the connection weights and biases, which enables ANN to generate outputs close to the target values. If the ranges of input and output data become normalized within 0–1, the ANN model will perform accurately. It is noteworthy that the outputs were within the range of 0–1, hence no need to normalize them. Therefore, only inputs were first normalized according to the following equation:

$$x_i = \frac{X_i - X_{\min}}{X_{\max} - X_{\min}} \tag{8}$$

where X_i is the ith data, $X_{\min}$ and $X_{\max}$ are the lowest and highest values in each case, respectively. Next, the total experimental data-sets (170 data) were randomized, and then 119 and 51 out of them were chosen for the training and testing, respectively. To avoid random initialization of the weights as well as random correlation, each run of the network was repeated three times. The mean square error (MSE) was used as the error function, which indicates the appropriateness of performance of the network based on the following equation:

$$\mathrm{MSE} = \frac{\sum_{i=1}^{i=N} \left(y_{i,\mathrm{predic}} - y_{i,\mathrm{exp}}\right)^2}{N} \tag{9}$$

where N is the total number of the data, $y_{i,\mathrm{predic}}$ is the predicted value, and $y_{i,\mathrm{exp}}$ is the ith experimental data.

3. Results and discussion

3.1. Optimization of three and four-layered ANNs

In the development of an ANN, a common problem is "overfitting", which is caused by the numerous free coefficients inside the network [27,28]. Extra training may lead to the overfitting of the network, i.e. the train set of data is learned precisely by the network, but thereby the network generalization is lost. Therefore, it is vital to test the network performance for the prediction of data, which have not been introduced to the network before. Hence, the testing and training processes were done simultaneously to assess the performance of the model without any overfitting. A set of the network coefficients, which obtain lowest MSE related to the testing data-set, can be considered as the most appropriate case [29]. It has been reported that 8–11 hidden layer neurons are able to provide a minimum value of the MSE [30]. Thereby, firstly, all designed networks were calibrated and tested using 10 neurons to find the best iteration number and then, using the best iteration, the numbers of hidden layer neurons were optimized. Table 4 shows the testing data-set MSEs related to the predicted values of the DE and EC by three-layered ANNs, which contain 10 neurons in their hidden layer, as a function of different iteration numbers. Also, at optimized iterations, the effect of hidden neuron numbers was tested with the related MSEs that have been presented in Table 5. From the applied point of view as well as high

Table 4
The MSE (×10^3) values of testing data-sets related to the DE and EC for the three-layered ANNs containing 10 neurons in their hidden layers, as a function of iteration number

	Model no. 1		Model no. 2		Model no. 3		Model no. 4		Model no. 5		Model no. 6	
Iteration number	EC	DE	EC	DE	EC	DE	EC	DE	EC	DE	EC	DE
20	1.706	31.179	1.702	4.814	3.230	13.186	3.230	13.186	0.272	26.556	0.389	2.776
50	1.723	14.212	0.838	3.630	1.170	8.409	1.934	4.648	1.015	17.149	0.335	2.429
80	0.718	8.838	0.838	3.630	0.719	6.584	1.547	5.369	0.337	9.845	0.204	1.952
100	0.751	4.569	0.369	3.723	0.599	5.619	0.404	3.242	0.669	18.716	0.106	2.822
200	0.625	4.855	0.224	2.993	0.427	6.237	0.167	3.438	0.600	19.950	0.047	4.516
400	0.277	7.837	0.393	2.062	0.457	5.420	0.344	2.507	1.706	50.594		
600	0.177	7.941	0.204	1.565	0.810	9.756	0.193	1.546				
800	0.271	11.029	0.225	1.675	0.553	10.089	0.176	2.051				
1,000			0.158	2.565	0.281	16.131	0.078	2.354				
1,200							0.600	3.303				
1,400							0.218	7.037				

importance of the DE criterion, the best model was chosen according to the lowest MSE obtained for the prediction of the criterion. It is observed that the optimums are varied from 80 to 600 and 9 to 11 for calibration iterations (Table 4) and hidden neuron numbers (Table 5), respectively. Based on the tables, a network with 10 hidden neurons and calibrated at 600th iteration, using the BFGS quasi-Newton back propagation (trainbfg) as the learning algorithm and tansig as the transfer functions, shows the lowest MSE (1.546×10^{-3}). Therefore, this model was applied for further study on the effect of hidden layers number on the ANN performance.

In this regard, a four-layered ANN (i.e. application of two hidden layers) was developed using the characteristics of the best three-layered ANN. Firstly, 10 hidden neurons were utilized and all the possibilities of their repartitions in the first and second hidden layers were examined. According to the presented results in Fig. 2, the lowest MSE of the testing data-set (1.5×10^{-3}) is related to the presence of four and six neurons in the first and second hidden layers, respectively. This means, the most suitable arrangement of the neuron number is in order of 5:4:6:2, which is related to the input layer (first and second) hidden layers, and output layer, respectively. Next, the effect of calibration iteration of the four-layered ANN was examined, and the results have been depicted in Fig. 3. The network showed the best performance (MSEs of 1.5×10^{-3} and 2.05×10^{-4} related to the predicted DE and EC) at the 600th iteration number. This iteration number is similar to the case found for the three-layered ANN and it can be

Table 5
The MSE (×10^3) values of testing data-sets related to the DE and EC for the three-layered ANNs calibrated at appropriate optimum iterations, as a function of hidden neuron number

	Model no. 1		Model no. 2		Model no. 3		Model no. 4		Model no. 5		Model no. 6	
Neuron number	EC	DE	EC	DE	EC	DE	EC	DE	EC	DE	EC	DE
6	4.465	13.683	0.242	3.987	0.548	10.885	0.166	2.747	0.449	11.003	0.350	4.227
7	0.562	9.662	0.314	2.083	0.362	12.264	0.261	3.028	0.767	9.486	0.378	2.587
8	0.668	6.648	0.301	2.265	0.526	12.949	0.186	3.002	0.353	7.216	0.136	2.694
9	0.645	3.619	0.154	1.680	0.371	7.693	0.219	2.698	0.478	4.383	0.098	2.166
10	0.751	4.569	0.204	1.565	0.457	5.420	0.193	1.546	0.337	9.845	0.204	1.952
11	0.388	4.382	0.245	2.446	0.108	4.645	0.207	1.808	0.445	41.009	0.044	2.994
12	0.476	4.820	0.256	2.075	0.704	6.662	0.244	1.783			0.066	4.940
13	0.469	6.006	0.091	2.503	1.705	29.731	0.062	2.653				
14			0.049	3.882			0.172	2.523				

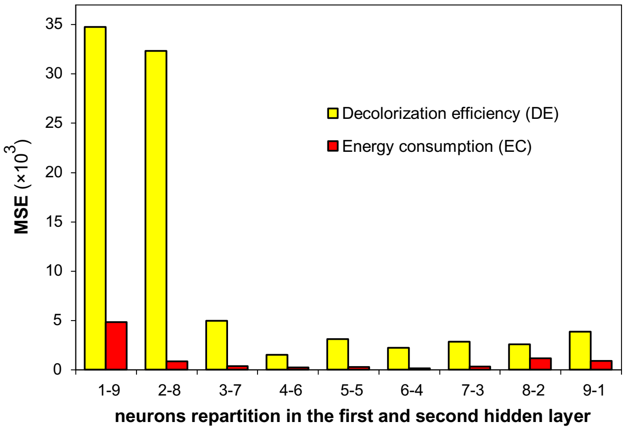

Fig. 2. Effect of the neuron number order (in the first and second hidden layers) on the testing data-set MSE.

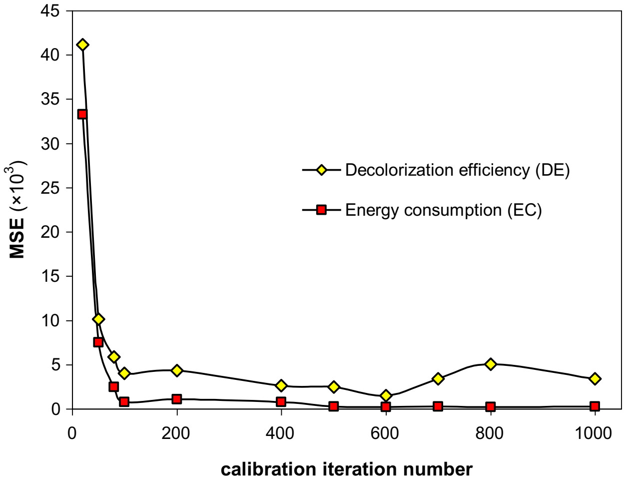

Fig. 3. Effect of calibration iteration on the testing data-set MSE for the four-layered ANN containing four and six neurons in the first and second hidden layers.

concluded that when the total neuron numbers are similar, the optimum iteration number is not dependent to the number of hidden layers.

Finally, by comparing the three- and four-layered ANNs, it is found that the latter is preferred to model the electrochemical process, due to the lower obtained MSE. A schematic diagram of the model is presented in Fig. 4.

3.2. K-fold cross-validation

The cross-validation is an approach to balance complexity with accuracy. To examine the four-layered model precisely, the K-fold cross-validation method was utilized. In this order, the total data-sets were subdivided into 17 equal-sized parts. The modeling was repeated 17 times, while at each time one of the data parts was used for testing. Average accuracy of the modeling was expressed by the correlation coefficient (R^2) and the MSE. The experimental and predicted output values of the testing data series, related to the DE and EC parameters, have been compared in Fig. 5. The MSE values for DE and EC simulations are 1.817×10^{-3} and 3.2×10^{-4}, respectively, which confirm the acceptable quality of the modeling. Also, Figs. 6–9 compare the simulated and experimental values of the DE and EC parameters as a function of NaCl concentration, applied voltage, initial pH, and the dye initial concentration. It can be found that under different operating conditions, the ANN model is able to simulate the process well.

3.3. Discussion on chemical aspects

It has been reported that NaCl is the most suitable case as supporting electrolyte [3]. The presence of chloride ions in the solution can significantly diminish the undesired impacts of other anions, such as HCO_3^-. The carbonate ions can precipitate Ca^{2+} or Mg^{2+} ions and form an insulating layer on the electrode surface. This layer increases ohmic resistance of the electrochemical cell, which in turn reduces the current and treatment efficiencies. Hence, the presence of chloride ions in the media is roughly recommended to conduct a normal operation of electrochemical treatment system [31]. Also, chlorine molecules are evolved via the anodic oxidation of chloride ions in aqueous media. The molecules are converted to hypochlorous acid and hypochlorite spices (Eqs. (1–5)), which are responsible for the destructive oxidation of organic pollutant compounds [32].

To optimize the NaCl amount in the electrolyte, several tests were conducted at a constant applied potential. Fig. 6(a) shows that increase in the NaCl amount up to 5 g/L, has promoted the DE (e.g. 92% after 18 min), and application of the further amounts has no considerable effect. Therefore, to avoid the usage of excess NaCl, an amount of 5 g/L NaCl was used in the subsequent experiments. Also, Fig. 6(b) shows that in the presence of 5 g/L NaCl, the increase in the EC parameter is not considerable during 18 min of the process.

The amount of applied voltage can alter the hypochlorite ions amount in the media and consequently can effect on the rate of electrochemical process. Dependency of the DE and EC parameters to the applied voltage variation has been presented in

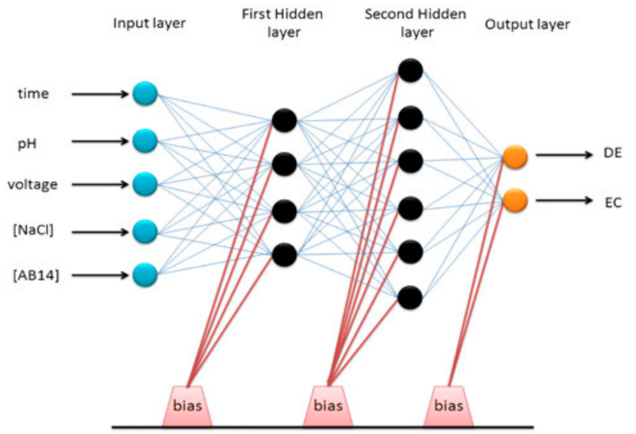

Fig. 4. Schematic view of the developed four-layered ANN model.

the Fig. 7(a) and (b). As it is observed, at the potential of 4 V, the process has reached to a considerable efficiency within 18 min of the process, while the consumed energy has still remained low. Therefore, this voltage was considered to be used in the process.

pH of the solution is another effective operational parameter in the electrochemical treatment processes. Depending on the pH, the electro-generated molecular chlorine can be disproportionated into HOCl and OCl^- ions according to the Eqs. (3) and (4) [3]. The oxidation potential of HOCl is more than OCl^-, hence, the electrochemical oxidation of organic pollutants in the presence of chloride ions shows a better performance in the acidic media [33]. Fig. 8 demonstrates the effect of pH on the DE and EC criteria. As it was expected, highest DE was obtained at the acidic

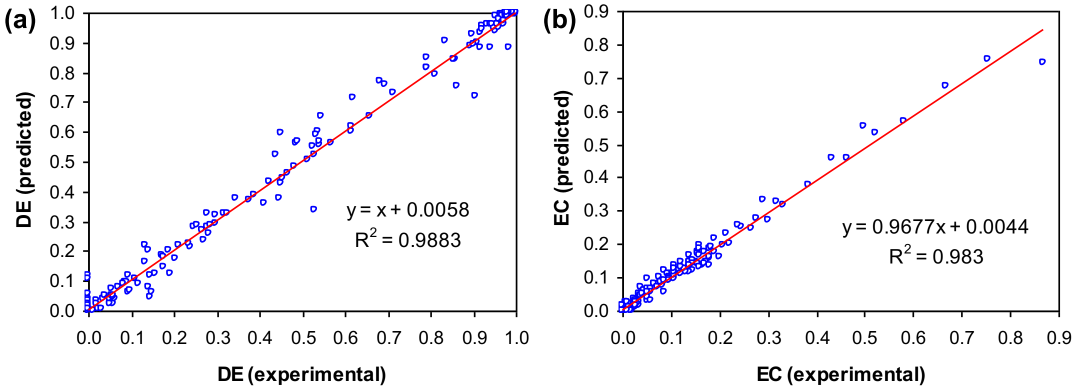

Fig. 5. Comparison of the experimental data and the predicted output values by four-layered ANN model; (a) is related to DE and (b) is related to EC.

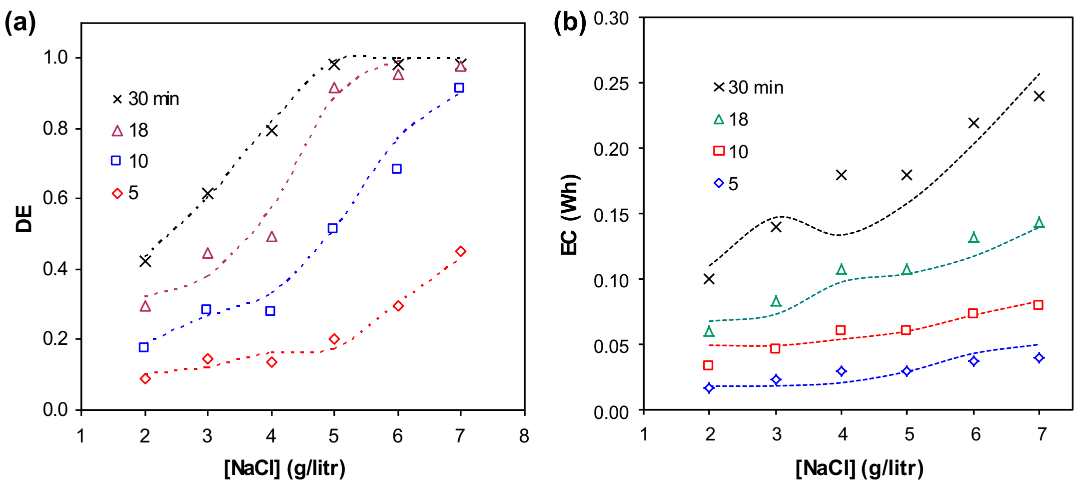

Fig. 6. Comparison of the experimental (symbols) and the ANN-predicted (dashed lines) values for DE (a) and EC (b) as a function of the supporting electrolyte concentration; $[AB14]_0 = 50$ mg/L, Voltage = 4 V, initial pH 6.4, and $T = 25$°C.

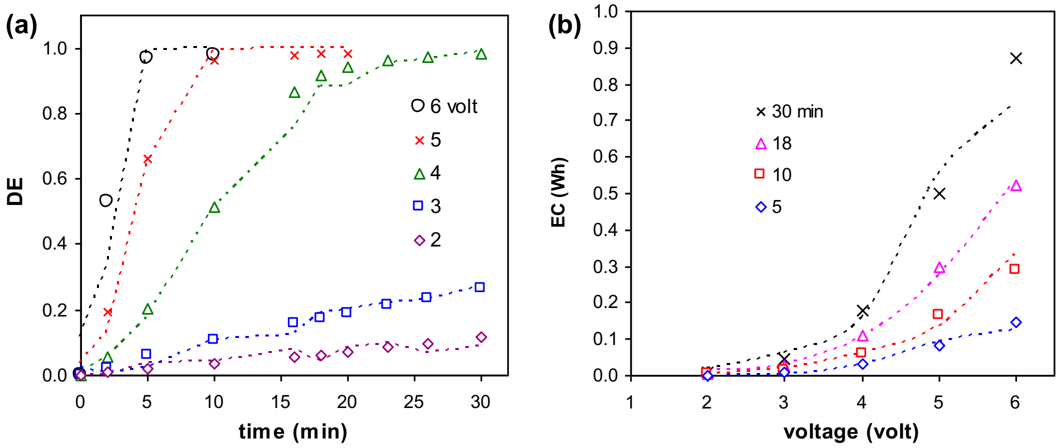

Fig. 7. Comparison of the experimental (symbols) and the ANN-predicted (dashed lines) values for the DE (a) and EC (b) as a function of applied voltage variation; $[\text{AB14}]_0 = 50\,\text{mg/L}$, $[\text{NaCl}] = 5\,\text{g/L}$, initial pH 6.4, and $T = 25\,^\circ\text{C}$.

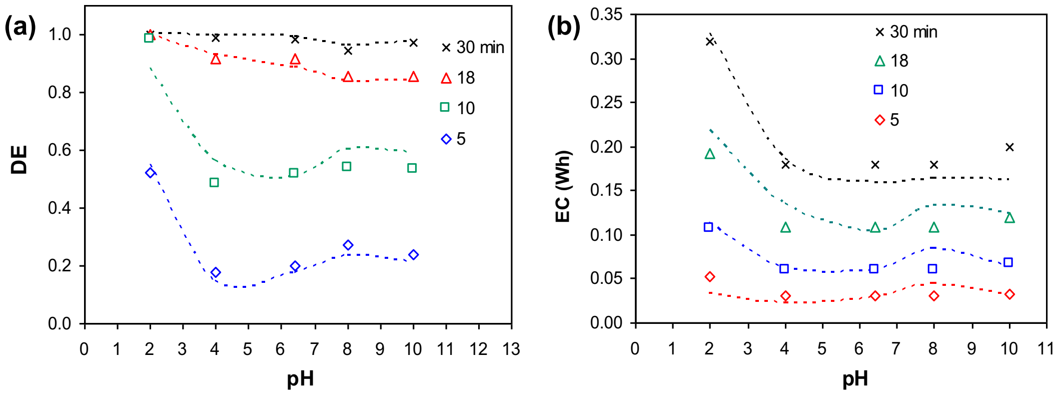

Fig. 8. Comparison of the experimental (symbols) and the ANN-predicted (dashed lines) values for the DE (a) and EC (b) as a function of pH variation; $[\text{AB14}]_0 = 50\,\text{mg/L}$, $[\text{NaCl}] = 5\,\text{g/L}$, Voltage = 4 V, and $T = 25\,^\circ\text{C}$.

pH of 2 and the increase in pH, has led to a mild decrease in the DE. Considering the low difference between the obtained DE at the pH 2 and the pH 6.4 (as the natural solution pH) after 18 min of the process and also considerably lower EC under pH of 6.4, this pH was selected as the process operational pH condition.

Influence of the initial dose of the pollutant on the DE and EC under the preferred process conditions has been shown in the Fig. 9. The DE is reduced when the pollutant dosage has been increased. This is the case, because under a certain oxidation ability of the electro chemical system, a decrease in the DE will occur if initial concentration of the pollutant is increased. Fig. 9(b) shows the EC variations vs. the obtained DE at different initial concentrations of the dye. As it can be seen, to obtain a higher efficiency, a higher energy is needed which is more considerable when the initial concentration of the dye is high.

3.4. COD assessment

The total amount of organic pollutants in a solution can be evaluated by the COD criterion [34]. Using this criterion, the extent of electro-oxidative mineralization of the pollutant was explored in this work. The obtained results showed that only 36% of organic contents of the dye solution have been mineralized after 18 min. It reveals that up to 18 min of the process, the active chlorine species (i.e. Cl_2, HOCl, and OCl^-) mainly are able to degrade the dye molecules into some colorless intermediates. Therefore, the electrochemical treatment process must be continued for longer times to achieve higher mineralization

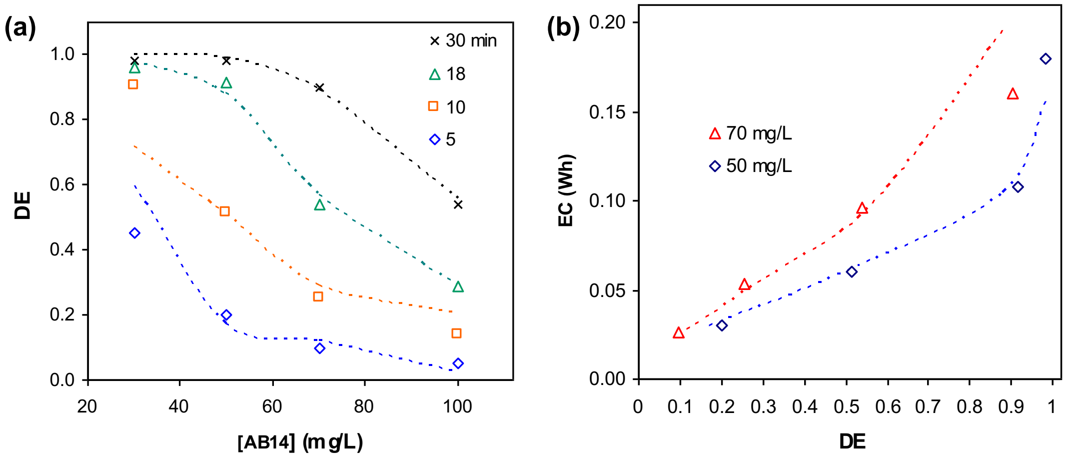

Fig. 9. Comparison of the experimental (symbols) and the ANN-predicted (dashed lines) values for the DE (a) and EC (b) as a function of the dye initial concentration; [NaCl] = 5 g/L, Voltage = 4 V, initial pH 6.4, and $T = 25$ ℃.

Table 6
The experimental characteristics of the electro-chemical treatment process

$[AB14]_0$ (ppm)	COD_0 (ppm O_2)	Optimum amount of the operation parameters							
		NaCl (g/L)	V (volt)	pH	I (Amper)	Process time (min)	DE	COD removal	EC (Wh/L)
50	49.6	5	4	6.4	0.1	18	92%	36%	0.24

efficiency [33]. This matter is in accordance with some related previous reports [35,36].

The experimental conditions and outcomes of the electrochemical treatment process have been summarized in Table 6.

4. Conclusions

In the present study, an electrochemical treatment process has been applied to treat AB14 aqueous solution, and the process was modeled using ANN methods. The obtained DE and EC were simulated based on five important effective parameters, such as reaction time, initial pH, applied voltage, supporting electrolyte, and the dye initial concentration. Briefly, the most important obtained results can be summarized as:

(1) Development of several various ANNs revealed that a four-layered feed-forward network, consist of trainbfg as the learning algorithm and tansig as the transfer function, has the best performance.
(2) The existence of four and six neurons in the first and second hidden layers, respectively, led to the best performance of the model, when the network was calibrated at 600th iteration.
(3) The K-fold cross-validation confirmed the goodness of the modeling. The MSE values of 1.817×10^{-3} and 3.2×10^{-4} and correlation coefficients of 0.9883 and 0.983 were related to the simulations of the DE and EC criteria, respectively.
(4) The experimental data showed the best conditions for the process performance as: 5 g/L of NaCl as the supporting electrolyte, applied potential of 4 V, and natural pH of 6.4.
(5) Under the above conditions, the efficiencies of decolorization and mineralization of the dye aqueous solution with an initial concentration of 50 mg/L, reached to 92 and 36%, respectively. The efficiencies were obtained during 18 min of the electrolysis process with a low consumed energy of 0.24 Wh/L.

References

[1] L. Fan, F. Yang, W. Yang, Performance of the decolorization of an azo dye with bipolar packed bed cell, Sep. Purif. Technol 34 (2004) 89–96.

[2] M. Muthukumar, M.T. Karuppiah, G.B. Raju, Electrochemical removal of CI acid orange 10 from aqueous solutions, Sep. Purif. Technol 55 (2007) 198–205.

[3] J. Basiri Parsa, M. Rezaei, A.R. Soleymani, Electrochemical oxidation of an azo dye in aqueous media investigation of operational parameters and kinetics, J. Hazard. Mater. 168 (2009) 997–1003.

[4] I. Yahiaoui, F. Aissani-Benissad, F. Fourcade, A. Amrane, Combination of an electrochemical pretreatment with a biological oxidation for the mineralization of nonbiodegradable organic dyes: Basic yellow 28 dye, Environ. Prog. Sustainable Energy 33 (2014) 160–169.

[5] I. Yahiaoui, F. Aissani-Benissad, K. Madi, N. Benmehdi, F. Fourcade, A. Amrane, Electrochemical pre-treatment combined with biological treatment for the degradation of methylene blue dye: Pb/PbO_2 electrode and modeling-optimization through central composite design, Ind. Eng. Chem. Res. 52 (2013) 14743–14751.

[6] S. Aber, N. Daneshvar, S.M. Soroureddin, A. Chabok, K. Asadpour-Zeynali, Study of acid orange 7 removal from aqueous solutions by powdered activated carbon and modeling of experimental results by artificial neural network, Desalination 211 (2007) 87–95.

[7] Y.-Y. Lau, Y.-S. Wong, T.-T. Teng, N. Morad, M. Rafatullah, S.-A. Ong, Coagulation–flocculation of azo dye Acid Orange 7 with green refined laterite soil, Chem. Eng. J. 246 (2014) 383–390.

[8] N. Daneshvar, A. Oladegaragoze, N. Djafarzadeh, Decolorization of basic dye solutions by electrocoagulation: An investigation of the effect of operational parameters, J. Hazard. Mater. 129 (2006) 116–122.

[9] J. Saien, A.R. Soleymani, Degradation and mineralization of direct blue 71 in a circulating upflow reactor by UV/TiO_2 process and employing a new method in kinetic study, J. Hazard. Mater. 144 (2007) 506–512.

[10] N. Daneshvar, S. Aber, V. Vatanpour, M.H. Rasoulifard, Electro-Fenton treatment of dye solution containing orange II: Influence of operational parameters, J. Electroanal. Chem. 615 (2008) 165–174.

[11] Y. Deng, J.D. Englehardt, Treatment of landfill leachate by the Fenton process, Water Res. 40 (2006) 3683–3694.

[12] L. Szpyrkowicz, C. Juzzolino, S.N. Kaul, A comparative study on oxidation of disperse dyes by electrochemical process, ozone, hypochlorite and Fenton reagent, Water Res. 35 (2001) 2129–2136.

[13] W.K. Jozwiak, M. Mitros, J. Kaluzna-Czaplinska, R. Tosik, Oxidative decomposition of Acid Brown 159 dye in aqueous solution by H_2O_2/Fe^{2+} and ozone with GC/MS analysis, Dyes Pigm. 74 (2007) 9–16.

[14] A.G. Vlyssides, D. Papaioannou, M. Loizidoy, P.K. Karlis, A.A. Zorpas, Testing an electrochemical method for treatment of textile dye wastewater, Waste Manage. 20 (2000) 569–574.

[15] A.G. Vlyssides, M. Loizidou, P.K. Karlis, A.A. Zorpas, D. Papaioannou, Electrochemical oxidation of a textile dye wastewater using a Pt/Ti electrode, J. Hazard. Mater. 70 (1999) 41–52.

[16] U.T. Una, U. Altay, A. Koparal, U.B. Ogutveren, Complete treatment of olive mill wastewaters by electrooxidation, Chem. Eng. J. 139 (2008) 445–452.

[17] D. Rajkumar, K. Palanivelu, Electrochemical treatment of industrial wastewater, J. Hazard. Mater. 113 (2004) 123–129.

[18] I. Yahiaoui, F. Aissani-Benissad, F. Fourcade, A. Amrane, Response surface methodology for the optimization of the electrochemical degradation of phenol on Pb/PbO_2 electrode, Environ. Prog. Sustainable Energy 31 (2012) 515–523.

[19] I. Yahiaoui, F. Aissani-Benissad, F. Fourcade, A. Amrane, Removal of tetracycline hydrochloride from water based on direct anodic oxidation (Pb/PbO_2 electrode) coupled to activated sludge culture, Chem. Eng. J. 221 (2013) 418–425.

[20] T.F. Edgar, D.M. Himmelblau, L. Lasdon, Optimization of Chemical Processes, second ed., McGraw-Hill, New York, NY, 2001.

[21] J. Peralta, G. Gutierrez, A. Sanchis, Design of artificial neural networks based on genetic algorithms to forecast time series, Adv. Soft. Comp. 44 (2007) 231–238.

[22] A.R. Soleymani, J. Saien, H. Bayat, Artificial neural networks developed for prediction of dye decolorization efficiency with UV/$K_2S_2O_8$ process, Chem. Eng. J. 170 (2011) 29–35.

[23] A. Durán, J.M. Monteagudo, M. Mohedano, Neural networks simulation of photo-Fenton degradation of reactive blue 4, Appl. Catal., B 65 (2006) 127–134.

[24] P. Kulkarni, S. Chellam, Disinfection by-product formation following chlorination of drinking water: Artificial neural network models and changes in speciation with treatment, Sci. Total Environ. 408 (2010) 4202–4210.

[25] A.J. Maren, C.T. Harston, R.M. Pap, Handbook of Neural Computing Applications, Academic Press, San Diego, CA, 1990.

[26] A.P.H. Association, Standard Methods for the Examination of Water and Wastewater, American Public Health Association, Washington, DC, 1268 (1998).

[27] J. Long, K. Xueyuan, H. Haihong, Q. Zhinian, W. Yehong, Study on the overfitting of the artificial neural network forecasting model, Acta Meteorol. Sin. 19 (2004) 216–225.

[28] S. Lawrence, A. Chung Tsoi, Lessons in neural network training: Overfitting may be harder than expected, in: Proceedings of the Fourteenth National Conference on Artificial Intelligence, California, CA, 1997, pp. 540–545.

[29] R. Hecht-Nielsen, Neurocomputing, Addison-Wesley Publishing Company, Reading, MA, 1990.

[30] S. Dutta, S.A. Parsons, C. Bhattacharjee, S. Bandhyopadhyay, S. Datta, Development of an artificial neural network model for adsorption and photocatalysis of reactive dye on TiO_2 surface, Expert Syst. Appl. 37 (2010) 8634–8638.

[31] H.M. Wong, C. Shang, Y.K. Cheung, G. Chen, Chloride assisted electrochemical disinfection, Proceedings of the Eighth Mainland-Taiwan Environmental Protection Conference, Tsin Chu, Taiwan 2002.

[32] C.R. Costa, P. Olivi, Effect of chloride concentration on the electrochemical treatment of a synthetic tannery wastewater, Electrochim. Acta 54 (2009) 2046–2052.

[33] C.R. Costa, F. Montilla, E. Morallón, P. Olivi, Electrochemical oxidation of acid black 210 dye on the boron-doped diamond electrode in the presence of phosphate ions: Effect of current density, pH, and chloride ions, Electrochim. Acta 54 (2009) 7048–7055.

[34] N. Daneshvar, M. Rabbani, N. Modirshahla, M.A. Behnajady, Photooxidative degradation of Acid Red 27 in a tubular continuous-flow photoreactor: Influence of operational parameters and mineralization products, J. Hazard. Mater. 118 (2005) 155–160.

[35] D. Rajkumar, B.J. Song, J.G. Kim, Electrochemical degradation of reactive blue 19 in chloride medium for the treatment of textile dyeing wastewater with identification of intermediate compounds, Dyes Pigm. 72 (2005) 1–7.

[36] A. Sakalis, K. Mpoulmpasakos, U. Nickel, K. Fytianos, A. Voulgaropoulos, Evaluation of a novel electrochemical pilot plant process for azodyes removal from textile wastewater, Chem. Eng. J. 111 (2005) 63–70.